Manuscript Title

Ultrasound Shear Wave Attenuation Imaging for Grading Liver Steatosis in Volunteers and Patients with Nonalcoholic Fatty Liver Disease: A Pilot Study

Authors:

Ladan Yazdani, MSc [1,2]

Iman Rafati, MSc [1,2]

Marc Gesnik, PhD [1]

Frank Nicolet, MSc [1]

Boris Chayer, M. Eng. [1]

Guillaume Gilbert, PhD [3,4]

Anton Volniansky, [4]

Damien Olivié, MD [4]

Jeanne-Marie Giard, MD, MPH [5]

Giada Sebastiani, MD [6]

Bich N. Nguyen, MD[7]

An Tang, MD, MSc [4,8]

Guy Cloutier, PhD, Eng. [1,2,4]

Affiliations:

[1] Laboratory of Biorheology and Medical Ultrasonics (LBUM), Centre de recherche du Centre hospitalier de l'Université de Montréal (CRCHUM), Montréal, Québec, Canada;

[2] Institute of Biomedical Engineering, Université de Montréal, Montréal, Québec, Canada;

[3] MR Clinical Science, Philips Healthcare Canada, Markham, Ontario, Canada;

[4] Department of Radiology, Radiation Oncology and Nuclear Medicine, Université de Montréal, Montréal, Québec, Canada;

[5] Department of Hepatology, Université de Montréal, Montréal, Québec, Canada;

[6] Division of Gastroenterology and Hepatology, McGill University Health Centre, Montreal, Quebec, Canada;

[7] Service of Pathology, Centre hospitalier de l'Université de Montréal (CHUM), Montréal, Québec, Canada;

[8] Laboratory of Clinical Image Processing, CRCHUM, Montréal, Québec, Canada.

Author Information:

Ladan Yazdani: Laboratory of Biorheology and Medical Ultrasonics, University of Montreal Hospital Research Center, 900 Saint-Denis, room R11-720, Montreal, Quebec, Canada, H2X 0A9, phone: 514-890-8000 #31423, fax: N/A, email: ladan.yazdani@umontreal.ca.

Iman Rafati: Laboratory of Biorheology and Medical Ultrasonics, University of Montreal Hospital Research Center, 900 Saint-Denis, room R11-720, Montreal, Quebec, Canada, H2X 0A9, phone: 514-890-8000 #31423, fax: N/A, email: iman.rafati@umontreal.ca

Marc Gesnik: Laboratory of Biorheology and Medical Ultrasonics, University of Montreal Hospital Research Center, 900 Saint-Denis, room R11-720, Montreal, Quebec, Canada, H2X 0A9, phone: 514-890-8000 #31423, fax: N/A, email: marc.gesnik@iconeus.com ; now at Iconeus, Paris 75014, France.

Frank Nicolet: Laboratory of Biorheology and Medical Ultrasonics, University of Montreal Hospital Research Center, 900 Saint-Denis, room R11-720, Montreal, Quebec, Canada, H2X 0A9, phone: 514-890-8000 #31423, fax: N/A, email: frank.nicolet@creatis.insa-lyon.fr; now at CREATIS, University of Lyon, France.

Boris Chayer: Laboratory of Biorheology and Medical Ultrasonics, University of Montreal Hospital Research Center, 900 Saint-Denis, room R11-720, Montreal, Quebec, Canada, H2X 0A9, phone: 514-890-8000-30309, fax: N/A, email: boris.chayer.chum@ssss.gouv.qc.ca

Guillaume Gilbert: MR Clinical Science, Philips Healthcare Canada, 1875 Buckhorn Gate, 5th floor, Mississauga, Ontario, Canada, L4W 5P1, phone: 438-998-4138, fax: N/A, email: guillaume.gilbert@philips.com

Anton Volniansky: Department of Radiology, Centre hospitalier de l'Université de Montréal (CHUM), 1000, rue Saint-Denis, Montreal, Québec, Canada, H2X 0C1, phone: N/A, fax: N/A, email: anton.volniansky.med@ssss.gouv.qc.ca

Damien Olivié: Department of Radiology, Centre hospitalier de l'Université de Montréal (CHUM), 1000, rue Saint-Denis, Montreal, Québec, Canada, H2X 0C1, phone: 514-890-8450, fax: N/A, email: damien.olivie@umontreal.ca

Jeanne-Marie Giard: Department of Hepatology, Université de Montréal, Montréal, Québec, Canada, H3T 1J4, 514/890-8000, fax: N/A, email: jeannemariegiard@gmail.com

Giada Sebastiani: Division of Gastroenterology and Hepatology, McGill University Health Centre, Montreal, Quebec, Canada, H2X 0C1, phone: 514-843-1616 , fax: N/A, email: giada.sebastiani@mcgill.ca

Bich N. Nguyen: Service of pathology, CHUM, 1051, rue Sanguinet, Montréal (Québec) H2X 0C1, phone: 514-890-8000 #21208, fax: N/A, email: bich.ngoc.nguyen.med@ssss.gouv.qc.ca

An Tang: Laboratory of Clinical Image Processing, CRCHUM, 900 Saint-Denis, Montreal, Quebec, Canada, H2X 0A9, phone: 514-890-8000 #11915, fax: N/A, email: an.tang@umontreal.ca

Guy Cloutier (Corresponding Author): Laboratory of Biorheology and Medical Ultrasonics, University of Montreal Hospital Research Center, 900 Saint-Denis, room R11-464, Montreal, Quebec, Canada, H2X 0A9, phone: 514-890-8000 #24703, fax: N/A, email: guy.cloutier@umontreal.ca, web: www.lbum-crchum.com

Funding information:

This work was supported in part by the Natural Sciences and Engineering Research Council of Canada under Grant 2022-03729, in part by the Canadian Institutes of Health Research under Grant 389385, and in part by the Oncotech consortium (Oncopole, Medteq, Transmedtech, Cancer Research Society, Fonds de Recherche Santé du Québec, and Siemens Healthcare) under Grant 293741. Salary award by the Fonds de recherche du Québec en Santé and Fondation de l'association des radiologistes du Québec (FRQS-FARQ #298509) was obtained by An Tang. Giada Sebastiani is supported by a Senior Salary Award from *FRQS* (#296306).

ELECTRONIC SUPPLEMENT

S1. Safety Usage of the Research Ultrasound Scanner in Shear Wave Elastography Mode

I. Introduction

The human liver imaging sequence developed for this study successively performed ultrasound transmissions and receptions [1]. **Fig. S1** shows the ultrasound sequence that included B-mode imaging, quantitative ultrasound imaging (QUS, not used in the current study), and 10 shear wave elastography (SWE) acquisitions.

First, conventional B-mode imaging was used to position the plane and the push location for SWE image acquisitions. The QUS mode allowed acquiring 30 radiofrequency (RF) images. Each image was obtained by compounding divergent wave images at 21 different angles (from -10° to 10°) at a frame rate of 150 per second.

Then, in the SWE mode, each acquisition included 10 SW propagation at the same depth but with different acoustic radiation force angles (-5° to 5°). The advantages of using 10 acquisitions with small angle differences are as follows:

1) Automatization of the 10 acquisitions: The technologist only had to set one push location (the 0° push), far away from blood vessels; then, the 10 acquisitions were made automatically by pushing near this location at small angles (ranging from -5° to 5° in polar coordinates), ensuring that they were far from blood vessels too. This simplified the acquisition process for users by reducing it to the click of a button.

2) Temporal consistency: Since there was no need to manually select 10 push zones in succession, the time between acquisitions and the process of saving each acquisition were reduced and performed automatically.

3) Security aspect: The pushes from successive acquisitions were generated in different directions, thereby limiting the amount of heating. This ensured additional safety during the procedure.

In summary, this approach simplified the acquisition process for technologists while maintaining consistency between acquisitions. Each push was made in a zone defined by the sonographer supervised by a clinical radiologist, ensuring that all pushes targeted the liver parenchyma and avoided major vessels.

Each SWE acquisition begun by focusing 5 pushes (992 cycles long, 357 µs long) at a given angle and 5 axially adjacent points with 3 mm distances in depth to produce a plane SW [2]. The focused push beams were transmitted by 64 elements of the transducer at a center frequency of 2.8 MHz. A radiology technologist positioned the first and last push locations to ensure that all of them targeted liver parenchyma and avoided major vessels. The same transducer was used to track SWs immediately after their propagation at a pulse repetition frequency (PRF) of 6,225 Hz. The propagation of SWs was then tracked by acquiring 100 frames made of ultrafast (2,083 frames per second) divergent waves. At the end of the sequence, the scanner was frozen. Parameters used in this sequence are presented in **Table S1**.

Measurements were made to make sure that the energy and acoustic pressure of B-mode, and SWE-mode met regulation standards. The chosen method was inspired by the work of Herman and Harris [3] and Palmeri *et al*. [4]. Shortly, the maximum of the peak rarefaction was measured using a hydrophone to determine the mechanical index (MI), and the intensity spatial peak temporal averaged (I_{SPTA}). The thermal index was computed from those maxima. MI indicates the ultrasound sequence's ability to cause cavitation-related bioeffects. I_{SPTA} corresponds to the maximum beam intensity averaged over the examination duration. The

thermal index corresponds to the quantification of the rise in tissue temperature that may occur during the examination [3, 4]. The food and drug administration (FDA) of the United States recommends to keep either the MI below 1.9 or the intensity spatial peak pulse averaged (I_{SPPA}) below 190 W/cm² [5, 6]. The limiting values for MI and I_{SPPA} are not independent; if either one of them falls below the designated FDA limit, then the other is permitted to exceed the limit [7]. The limit for the I_{SPTA} is 720 mW/cm² as elastography complies with track 3 in [5, 6, 8], while the thermal index must remain under 6 °C [4, 5]. In this work, MI, I_{SPTA}, and thermal index were assessed to investigate the compliance with FDA limits. The maximal sonication power was then limited for the safety of volunteers and patients, and approved by the institutional review board of the Centre de recherche du Centre Hospitalier de l'Université de Montréal (CRCHUM).

II. Acoustic Measurements

MI, I_{SPTA}, and the thermal index were determined for the selected imaging sequence. A membrane hydrophone (HMB-0200, ONDA Corp., Sunnyvale, CA, USA) connected to a digital oscilloscope (CompuScope 12501, Vitrek LLC, Lockport, IL, USA) was positioned at the bottom of a double-distilled deionized water tank. The research ultrasound system (Verasonics Vantage, Kirkland, WA, USA) was connected to the ATL C5-2 clinical probe (Philips Healthcare, Andover, MA, USA). The 100 MHz hydrophone sampled signals were converted to sound pressure (Pascal) using the sensitivity of the hydrophone at 2.8 MHz (196 mV/Pa). The ultrasound probe was attached to a computer-controlled multi-axis robotic system (ACR9000, Parker Hannifin Corp., Rohnert Park, CA, USA) to localize the maximum pressure position. Because acoustic power measurements were made in a water tank and not in an attenuating tissue environment, the FDA recommends to compensate the attenuation by using a derating

attenuation factor of α = 0.3 dB.MHz^{-1}.cm^{-1}. The perpendicularity between the hydrophone and the probe was aligned manually using the real-time focused B-mode.

A dedicated pressure measurement strategy was programmed using Matlab (Mathworks, Natick, MA, USA) to synchronise Verasonics sequence transmissions during hydrophone measurements. Transmitted voltages of 10, 20, 30, 40, and 50 V were studied for a focus distance between the probe and the location of the push of 20, 30, 40, 60, and 80 mm. SWE acoustic pressure measurements included 50 cycles pushes instead of 992 cycles to prevent hydrophone damage (as the amplitude of pushes is constant, this did not impact the identification of the peak rarefaction maximum). Every ultrasound emission was repeated 16 times for averaging purpose. Because acoustic outputs in SWE-mode are much higher than in B-mode or QUS-mode, results given next correspond to the SWE sequence component.

III. Results

1. Mechanical Index (MI)

MI as a function of focus depths and selected voltages for a derating value of 0.3 dB.MHz^{-1}.cm^{-1} is presented in **Fig. S2**. To stay below the FDA limit of 1.9, the maximum voltage for SWE measurements at depths $\geq$ 40 mm was limited to 42 V. For smaller depths, the voltage was limited to 25 V (**Table S2**). For comparison, MI in B-mode with parameters of **Table S1** was 0.28.

2. Intensity Spatial Peak Temporal Averaged (I_{SPTA})

I_{SPTA} results as a function of depth are given in **Fig. S3** for selected voltages in **Table S2**. For every acoustic radiation force depth, I_{SPTA} was lower than the FDA threshold of 720

mW/cm^2. This was achieved by adjusting the delay between the 10 SWE repetitions. In B-mode, it was 6.15 mW/cm^2.

3. Thermal Index

Fig. S4 presents the estimated thermal index in soft tissues of the SWE sequence as a function of depth for voltages in **Table S2**. For every push focus depth, the index was close to 4 ^{o}C and below the FDA threshold of 6 ^{o}C. The estimated thermal index in B-mode using the parameters of **Table S1** was 0.09 ^{o}C.

IV. Discussion

The result in **Fig. S2** showed that the research ultrasound system could exceed FDA safety criteria when the selected voltage was not constrained within a safe range for given acoustic radiation force depths. SWE pushes are particularly at risk of overrunning FDA limits since they combine the use of focused waves, high voltages, and several hundreds of emitted cycles.

According to the FDA, compliance with the restriction of MI and I_{SPTA} is sufficient to limit the risk from acoustic output exposure levels [5, 6]. These two parameters are below the FDA limits based on the results in **Fig. S2** and **Fig. S3**. As also reported, the thermal index is not well suited for the acoustic radiation force imaging (ARFI) and SWE imaging modalities [9, 10]. According to [11], for the thermal index of 4, the maximum safe duration of examination without thermal risk would be 15 seconds, while all liver imaging sequence in this work lasted less than 10 seconds. Furthermore, as each SWE repetition uses a different radiation angle, diffusion can occur and reduce the heating inside the liver [12]. Thermal index values were presented here for informative purpose only. Throughout our sequence design process, safety margins have

been added to the various parameters of the sequence to respect the principle of ALARA (as low as reasonably achievable). By fixing the maximum voltage at a given depth, the sequence used for this NAFLD human study met all safety criteria recommended by the FDA. By applying the ALARA principle, it was decided to lengthen delays between SWE acoustic radiation force pushes to reduce the frame rate, and to change the angle between the 10 consecutive push lines to increase the safety for human liver scanning. In addition, it took about one minute to save RF data after running the sequence. During data saving, no ultrasonic emissions were possible, further reducing the risk of thermal overheating.

S2. Ultrasound Shear Wave Data Acquisition and Parameter Computation

I. Shear Wave Attenuation (SWA)

The revisited frequency shift (R-FS) method was used for SWA computation [13]. This algorithm assumes the amplitude spectrum of SWs to be proportional to a gamma density distribution. If a SW has a frequency spectrum $S(f)$ at a lateral distance x_0, then:

$$|S(f)| \propto f^{k_0-1} e^{f\beta_0}$$

where f is the SW frequency, and k_0 and β_0 are the shape and rate parameters of the gamma function, respectively. The attenuation coefficient (α) was computed by fitting the gamma spectrum at a lateral distance Δx, and finding the slope of the rate parameter with respect to Δx (*i.e.*, $\beta(\Delta x) = \beta_0 + \alpha \Delta x$) [13]. Both the shape and rate parameters are allowed to vary with the R-FS method, and the adaptive random sample consensus (A-RANSAC) algorithm was used for line fitting [13]. Two examples of line fitting of the rate parameter for SWA computation are shown in **Fig. S5** (panels a and b).

Ten SWA maps were reconstructed from each acquisition by applying the R-FS method on the defined ROI. SWA coefficients were averaged on each pixel using images with gamma fitting providing coefficients of determination R^2 >0.8 or larger. The averaging procedure for obtaining the final attenuation map is shown in **Fig. S6**.

II. Shear Wave Dispersion (SWD)

SWD was estimated as the slope of the SW phase velocity versus frequency, according to [14, 15], on the same ROI as SWA computations by averaging the velocity field over depth. The A-RANSAC method was used for line fitting and for finding the slope. Two examples of line fitting of SW phase velocity are shown in **Fig. S5** (panels c and d). The SWD was computed between averaged values of the lower frequency at half maximum (67 Hz) and peak frequency (110 Hz), determined *a posteriori* on the whole dataset. For a given acquisition, SWD values were estimated from ten SW records, and the mean and standard deviation (SD) were computed for line fittings with R^2 > 0.8 or larger.

Electronic Supplement References

1. Deng Y, Rouze NC, Palmeri ML, Nightingale KR. Ultrasonic shear wave elasticity imaging sequencing and data processing using a Verasonics research scanner. IEEE Trans. Ultrason. Ferroelectr. Freq. Control. 2017; 64:164-176
2. Bercoff J, Tanter M, Fink M. Supersonic shear imaging: a new technique for soft tissue elasticity mapping. IEEE transactions on ultrasonics, ferroelectrics, and frequency control 2004; 51(4): 396–409.
3. Herman BA, Harris GR. Models and regulatory considerations for transient temperature rise during diagnostic ultrasound pulses. Ultrasound Med. Biol. 2002; 28:1217-1224

4. Palmeri ML, Frinkley KD, Nightingale KR. Experimental studies of the thermal effects associated with radiation force imaging of soft tissue. Ultrason. Imaging 2004; 26(2):100-114
5. Food and Drug Administration. Information for manufacturers seeking marketing clearance of diagnostic ultrasound systems and transducers. 2008; 1–64
6. Food and Drug Administration. Marketing clearance of diagnostic ultrasound systems and transducers: Guidance for industry and food and drug administration staff. Food Drug Admin., Silver Spring, MD, USA, Tech. Rep. FDA-2017-D-5372, 2019.
7. Duck AF. Safety standards and regulations: the manufacturers' responsibilities. In: Haar G, editor. The safe use of ultrasound in medical diagnosis (3rd Ed.), London, United Kingdom, The British Institute of Radiology 2012; 134–142
8. Miller DL, Abo A, Abramowicz JS, et al. Diagnostic ultrasound safety review for point-of-care ultrasound practitioners. J Ultrasound Med. 2020; 39:1069-1084
9. Church CC, Labuda C, Nightingale K. A. Theoretical study of inertial cavitation from acoustic radiation force impulse imaging and implications for the mechanical index. Ultrasound Med Biol. 2015; 41:472-485
10. Bigelow TA, Church CC, Sandstrom K, et al. The thermal index: its strengths, weaknesses, and proposed improvements. J. Ultrasound Med. 2011; 30: 714-734
11. Ziskin MC. The thermal dose index [published correction appears in J. Ultrasound Med. 2010; 29(12):1854]. J. Ultrasound Med. 2010; 29:1475-1479
12. Nightingale K. Acoustic radiation force impulse (ARFI) imaging: a review. Curr Med Imaging Rev. 2011; 7:328-339

13. Yazdani L, Bhatt M, Rafati I, Tang A, Cloutier G. The revisited frequency-shift method for shear wave attenuation computation and imaging. IEEE Transactions on Ultrasonics, Ferroelectrics, and Frequency Control 2022; 69:2061-2074
14. Barry CT, Mills B, Hah Z et al. Shear wave dispersion measures liver steatosis. Ultrasound in Medicine and Biology 2012; 38:175-182
15. Parker KJ, Partin A, Rubens DJ. What do we know about shear wave dispersion in normal and steatotic livers? Ultrasound in Medicine and Biology 2015; 41:1481-1487

Electronic Supplement Tables

Table S1— Programmed parameters of the ultrasound sequence for human liver imaging.

Mode	Wave duration (μs)	Wave frequency (MHz)	Wave cycles	PRF (Hz)	Compounding (number of angles)	Focus depth (mm)	Frame rate (s^{-1})	Wave amplitude (volts)
B-mode	0.64	3.125	2	1280	64	50	20	20
Diverging wave QUS	0.64	3.125	2	3145	21	NA	150	30
SWE push	357	2.778	992	2793	5	20-80	N/A	25 or 42
Diverging wave SWE tracking	0.64	3.125	2	6225	3	NA	2083	30

PRF: pulse repetition frequency, QUS: quantitative ultrasound, SWE: shear wave elastography.

Table S2— The voltage used for shear wave elastography (SWE) pushes at different user selected push depths for human liver imaging.

Focus distance	20 mm	30 mm	40 mm	60 mm	80 mm
Voltage	25 V	25 V	42 V	42 V	42 V

Electronic Supplement Figures

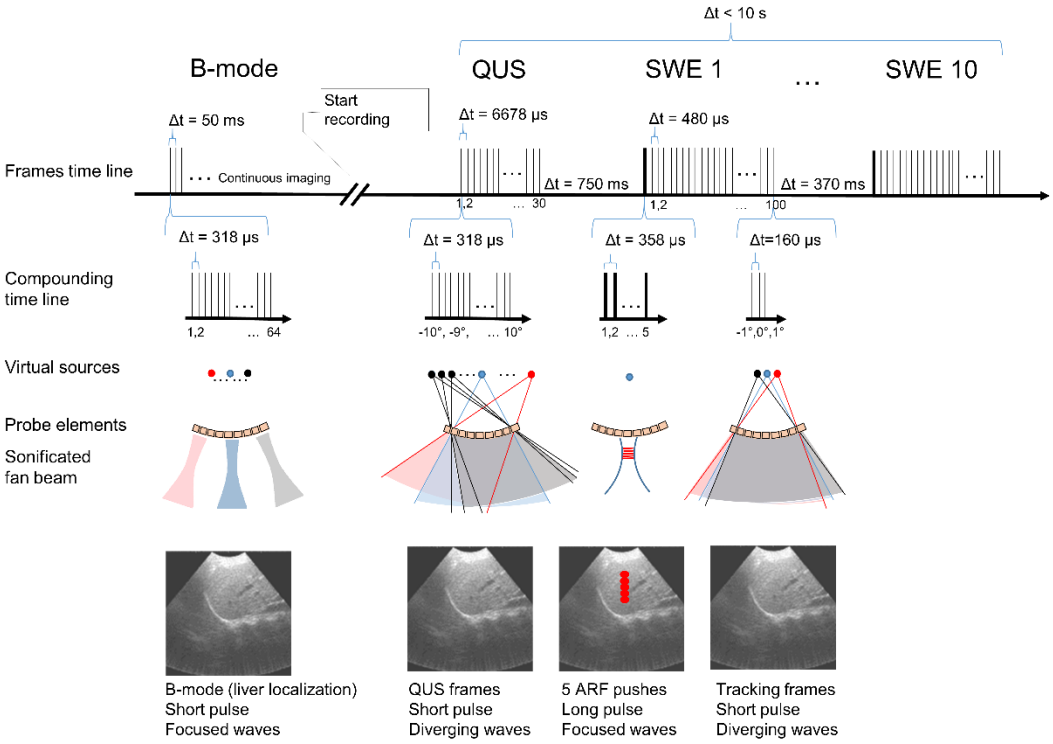

Fig. S1— Schematic of the human liver imaging sequence. ARF: acoustic radiation force, QUS: quantitative ultrasound, SWE: shear wave elastography.

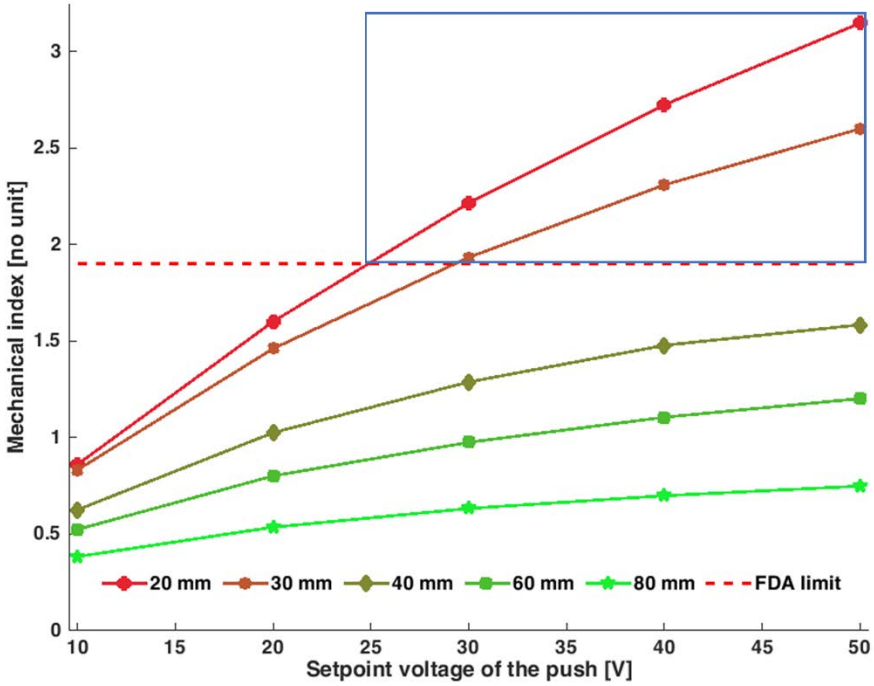

302

303 **Fig. S2—** Measured mechanical index (MI) in shear wave elastography (SWE) mode as a
304 function of the selected voltage for different focus depths using a hydrophone in a water tank.
305 A derating attenuation value of 0.3 $dB.MHz^{-1}.cm^{-1}$ was considered for those measurements.
306 The MIs and voltages in the blue box had never been used for human acquisitions.

307

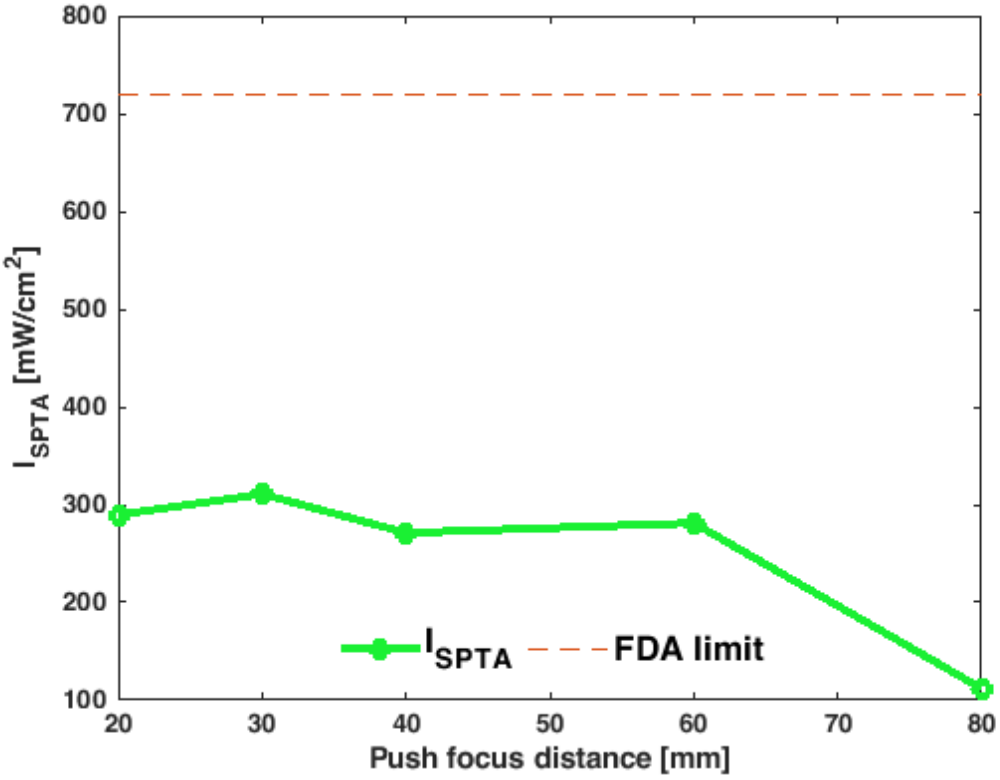

Fig. S3— Measured intensity spatial peak temporal averaged (I_{SPTA}) in mW/cm^2 as a function of the focus depth for the maximum selected voltage limit (**Table S2**) programmed on the Verasonics system for human liver imaging.

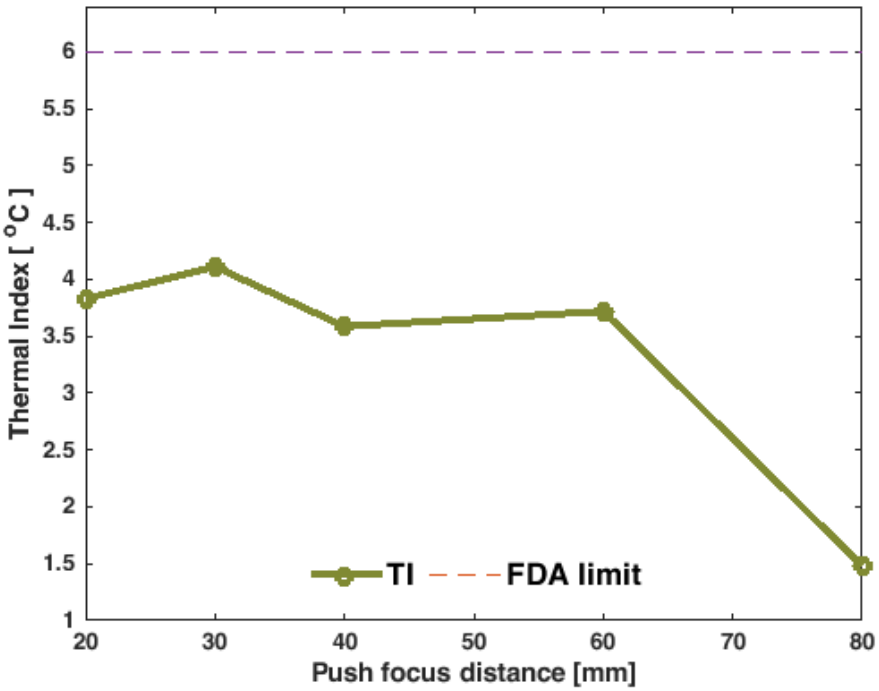

315

316 **Fig. S4—** Estimated thermal index (TI) in ºC as a function of the focus depth for the maximum
317 selected voltage limit (**Table S2**) programmed on the Verasonics system for human liver
318 imaging.

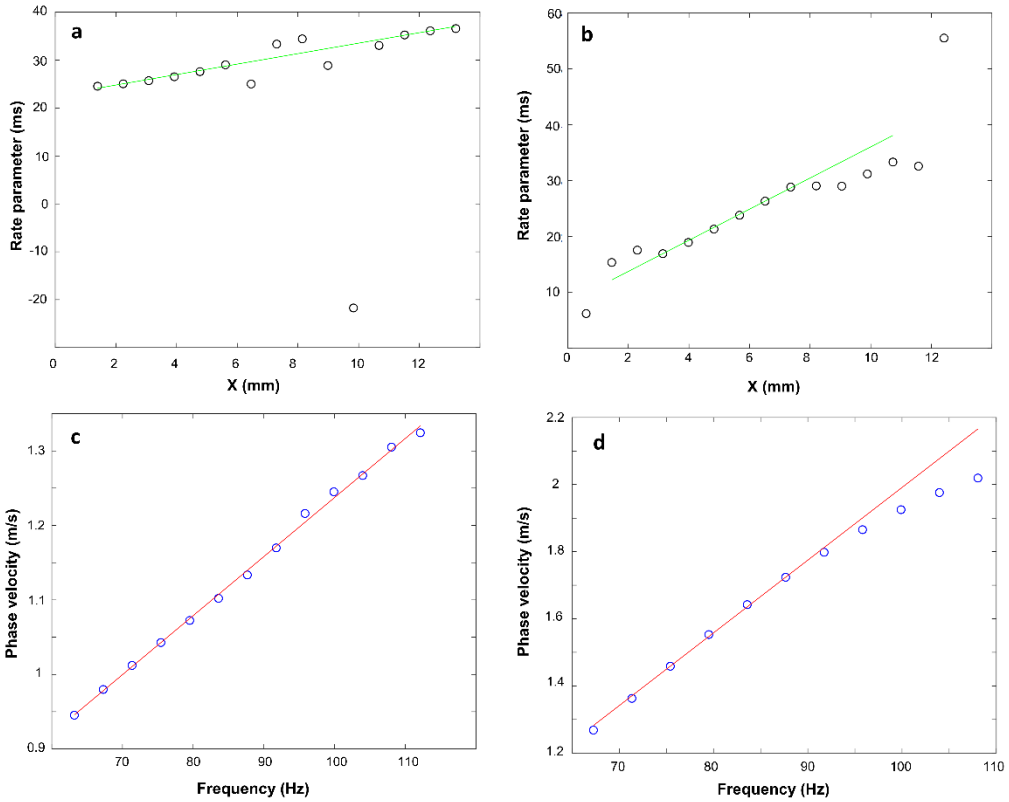

Fig. S5— Examples of shear wave attenuation and shear wave dispersion line fittings using A-RANSAC for one volunteer and one NAFLD patient (top and bottom rows represent line fitting of the rate parameter of the gamma distribution versus lateral distance for SWA computation, and line fitting of the phase velocity versus frequency for SWD computation, respectively). (a) 30-years-old healthy volunteer woman (R^2 of the fitted line=0.97), (b) 62-years-old man with steatosis grade 2, lobular inflammation grade 2, ballooning grade 2, fibrosis stage 4 (R^2=0.87), (c) 32-year-sold healthy volunteer man (R^2=1), and (d) 60-years-old woman with steatosis grade 3, lobular inflammation grade 3, ballooning grade 2, fibrosis stage 3 (R^2=0.95).

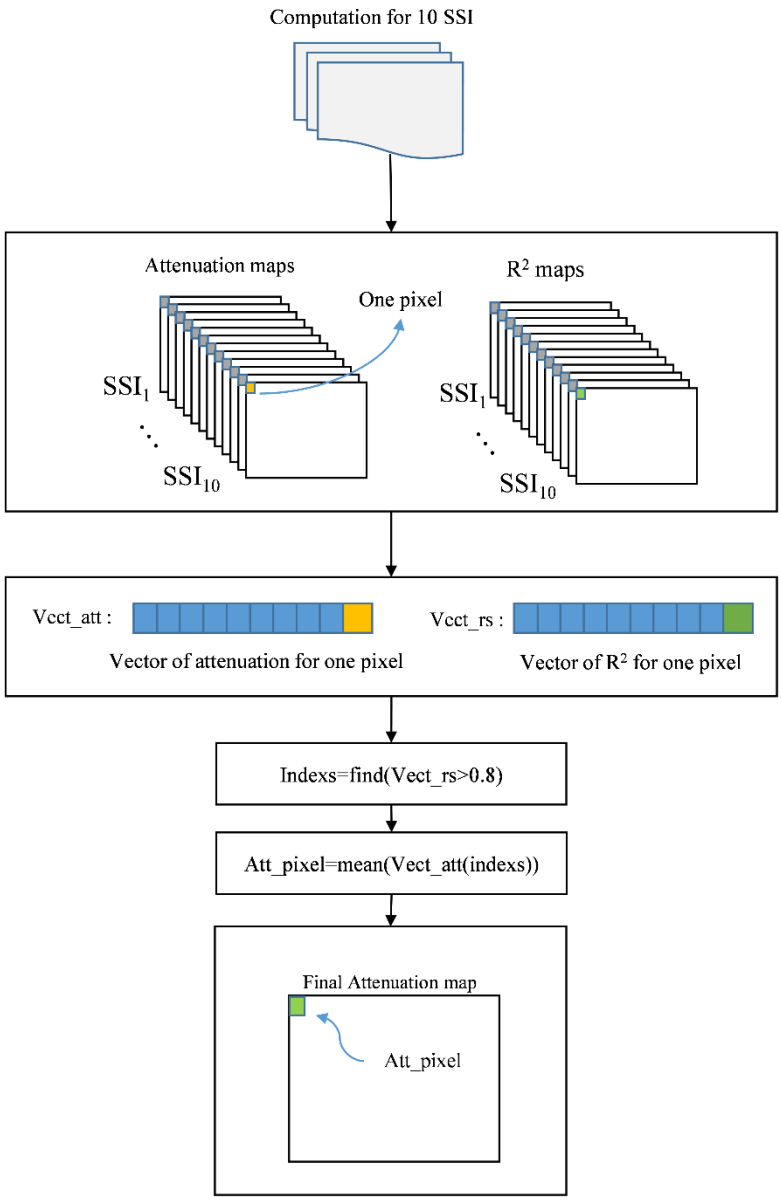

328

329 **Fig. S6—** The averaging procedure over the 10 acquisitions (SSI represents shear wave

330 acquisitions with different angles of pushes lines).